Optimization of the Electromagnetic Characteristics of a 3-Phase Squirrel-Cage Induction Motor Using FEM

Gyftakis, K.N. , Katsantonis , I. and Kappatou, J.

Journal of Materials Science and Engineering A 4 (3) (2014) 65-72

Optimization of the Electromagnetic Characteristics of a 3-Phase Squirrel-Cage Induction Motor Using FEM

Konstantinos N. Gyftakis, Ioannis Katsantonis and Joya Kappatou

Laporatory of Electromechanical Energy Conversion, Department of Electrical and Computer Engineering, University of Patras, University Campus, Rion, GR-54124, Greece

Received: February 13, 2014 / Accepted: March 01, 2014 / Published: March 10, 2014.

Abstract: The induction motor due to its characteristics forms the most common choice of industrial applications worldwide. In this work, with the use of FEM analysis, a specific induction motor is optimized under three different criteria. The geometric features of the rotor compose the designing variables of the optimization process. Three models have been created and studied. These resulting models present optimized electromagnetic characteristics depending on the designer's restrictions and also on the application requirements. The finite element analysis carried out is AC steady-state and takes into consideration the non-linear characteristic of the stator and rotor iron core.

Key words: Induction motor, FEM analysis, optimization.

1. Introduction

The Induction motor forms the 85% of industrial applications, due to its simple manufacturing, reliability and steadiness. Far more than 95% of an electric motor life cycle cost is energy cost [1]. Substantially, reducing motor losses will have a significant impact on one country's energy consumption [2]. Induction motor design principles have not changed dramatically over the years, while the tools and knowledge of the engineers have improved considerably. Extensive research has been carried out in the last years aiming to high efficiency motors through the optimization of the motors design characteristics [3-5]. Together with the development of the computer's science, FEM has also been developed and extensively used by researchers to aid in such problems [6-8].

The optimization of the motor geometry has the second greater impact between the possible areas for the improvement of the induction motors performance, after the improvement of the active material. Besides that, it is worldwide the least cost-consuming method of induction motors improvement [1]. Firstly, the design optimization process is carried out with the use of simulation models under computer analysis, in order to reshape the motors blueprints. Then, the optimized motor is manufactured. It is obvious that the cost of the process described above, is extremely low while the cost of the manufacturing process remains at the same level.

It is well known that every motor designer confronts a significant dilemma while designing an induction motor [9]. If the rotor's resistance is high then the motor's starting torque will be high and the starting current low. On the other hand, the pullout torque occurs at a higher slip causing less part of the air-gap power to transform into mechanical power and consequently reduction of the motor's efficiency. An induction motor with low rotor resistance presents low starting torque and great starting current but its efficiency under normal load is high. So, an induction

Corresponding author: Konstantinos N. Gyftakis, research fields: electrical machines design and FE analysis and fault diagnosis. E-mail: kosgyftak@upatras.gr.

motor designer is obliged to choose between the following two conflicting demands, depending on the application: Improved starting performance or high efficiency. NEMA (National Electrical Manufacturing Association) has divided induction motors in four classes (A, B, C, D), depending on the rotor's geometrical characteristics [10].

In this work, a 3-phase, 4 kW, 400 V cast aluminum induction motor with 36 stator and 28 rotor slots has been simulated with the software OPERA Electromagnetic Fields. This first model has been created so that the geometric variables of the rotor are parameterized. The parameterized model has been optimized under three different criteria, covering every possible application with the use of the Optimizer, which is an application of the OPERA. In these three optimization processes, all the parameterized geometric variables of the rotor are taken into account. The first of these three processes occurred to a model with optimized starting behavior, whereas the second to a model with optimized mechanical output power at nominal speed and the third to a model with optimized efficiency at nominal speed. In all simulations, the electromagnetic analysis was 2D AC steady-state. The analysis considers the models non-skewed and takes into account the non-linear B-H magnetic characteristics of the stator and rotor iron core. The stator resistance used in the analysis, was measured by DC current injection in the real induction motor.

The purpose of this work is: by keeping the stator intact, to acquire new rotor geometries which will lead to the production of motors with optimized some electromagnetic characteristics, depending on the application requirements. For an induction motor manufacturer this means that, practically with the same production cost, improved motors can be produced, exploiting the results from FEM optimization analysis. Also, faster and cheaper production of models under special client requirements can be achieved, under minimum new designing process.

2. Simulation of the Original Model

2.1 Designing the Model

The motor chosen to be simulated is a 3-phase asynchronous cast aluminum squirrel cage induction motor, 4 kW, 400 V, with 36 stator slots and 28 rotor slots. The stator windings resistance was measured in the laboratory by DC current injection in two phases of the motor. In Fig. 1, the stator and rotor of the original motor are presented.

The simulated model has to be parameterized in order to be able to modify its geometrical characteristics. This means that, while designing the model, the geometrical features of the motor are inserted in the simulation software as variables. In this work, the optimization process takes into account the rotor geometrical variations. So, Fig. 2 shows that the basic rotor variables which are taken into account through the optimization. The depth of the rotor bar is controlled through the variable A. The variable C shows the width of the rotor bar. Variables D and E concern the rotor slot width and opening respectively. Finally, the shape of the bottom of the rotor bar is given by the variable B.

Furthermore, in the following Fig. 3 one can see the whole simulated model of the original induction motor.

(a) (b)

Fig. 1 The main parts of the original induction motor: (a) the rotor and (b) the stator.

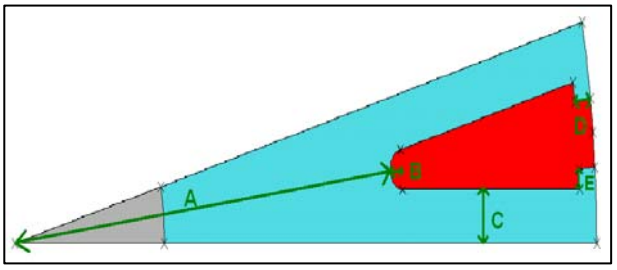

Fig. 2 The rotor geometric variables.

Through external circuits, the three phases of the stator form a delta wound, supplied by a 3-phase 380 V voltage system, according to the manufacturer's blueprints.

2.2 Analysis and Results of the Original Model

The analysis carried out in this work is AC time harmonic. The analysis takes into account the non-linear magnetic characteristics of the stator and iron core. Also, the skin effect in the rotor bars has been taken into consideration by the appropriate creation of the model's mesh. In Fig. 4, one can see the spatial distribution of the magnetic field at starting (Fig. 4a) and at nominal speed (Fig. 4b). As expected, during the starting the field lines do not penetrate deep into the rotor core because of the iron saturation and the creation of the leakage flux field. Moreover, the four magnetic poles of the motor can easily be observed in both cases.

The electromechanical characteristics of the simulated model are presented in Table 1.

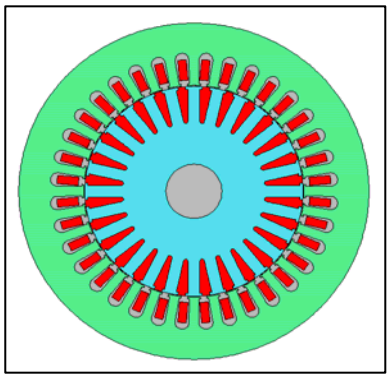

Fig. 3 The simulated model of the original induction motor.

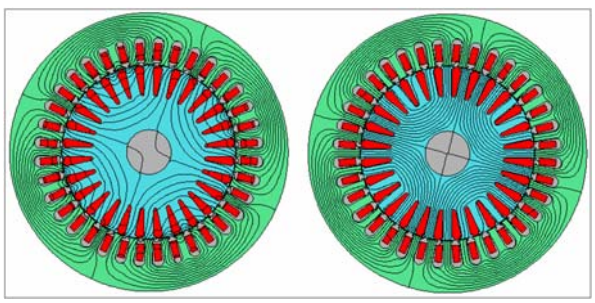

(a) (b)

Fig. 4 The spatial magnetic field distribution: (a) at starting and (b) at nominal speed.

Finally, the current density amplitude along the depth of a rotor bar is presented at starting in Fig. 5. The skin effect is clearly present in this case. The amplitude of the current density is much greater at the surface of the rotor bar causing the increase of the bar's resistance.

3. Optimization of the Motor's Starting Behaviour

In this case, the motor's starting electromagnetic characteristics will be optimized. The optimization analysis takes into account all the geometric variables of the rotor. The model which occurred for this optimization case is presented in Fig. 6.

The geometric rotor variables of the original model and the model with optimized starting behavior are presented in Table 2, for comparison. The depth of the rotor bar, as a consequence of the changes in A and B variables, has strongly been reduced. There is also a significant decrease of the width of the rotor bar (variable C). Variables D and E concern the rotor slot

Table 1 Electromechanical results of the original simulated model.

Starting Torque (Nm)	41.04
Starting Stator Current (A)	37.23
Torque at nominal speed (Nm)	26.91
Stator Current at nominal speed (A)	7.54
Input Power (W)	5038.14
Output Power (W)	4055.34
Power factor cosφ	0.83
Efficiency η (%)	80.49

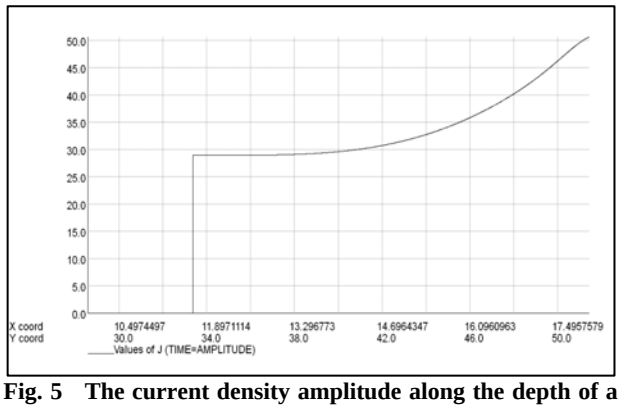

Fig. 5 The current density amplitude along the depth of a rotor bar in A/mm^2.

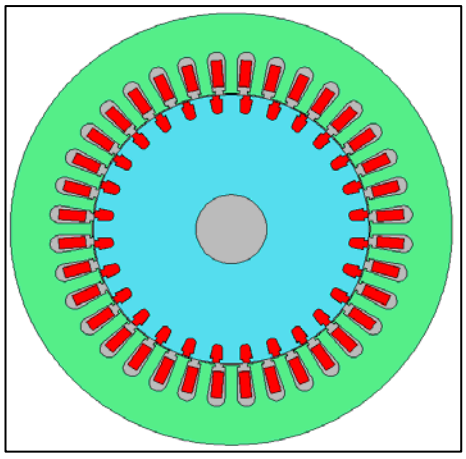

Fig. 6 The model with optimized starting behavior.

Table 2 The geometric rotor variables of the original and the model with optimized starting behavior.

Design variables	A	B	C	D	E
Original model	35.35	2.2	3	1.5	1.1
Optimized model	46.9	2.03	3.45	1.67	1.0

width and opening respectively. The first one has increased, while the second has decreased. The changes in A, B and D design variables concern the bar resistance. The optimized model has greater bar resistance. The changes on the design variables D and E have resulted to a model with greater slot opening and greater iron width at the slot, provoking a greater harmonic content in the magnetic field of the air gap.

The characteristics of the torque and stator current versus speed for the two models studied are presented in Figs. 7 and 8, respectively. One can observe (Fig. 7), that the starting torque of the optimized model is 45% greater than the one of the original model. Moreover, both the optimized model's pullout torque occurs at lower speed causing greater stability area, but on the other hand, 41% lower output power at nominal speed. Furthermore, in Fig. 8 the optimized model's stator current is much lower than the original model's for every speed.

The model, which resulted from this optimization process, is a NEMA's class D motor. It could be used for applications such as punch presses and shears, or any application which requires frequent start-ups.

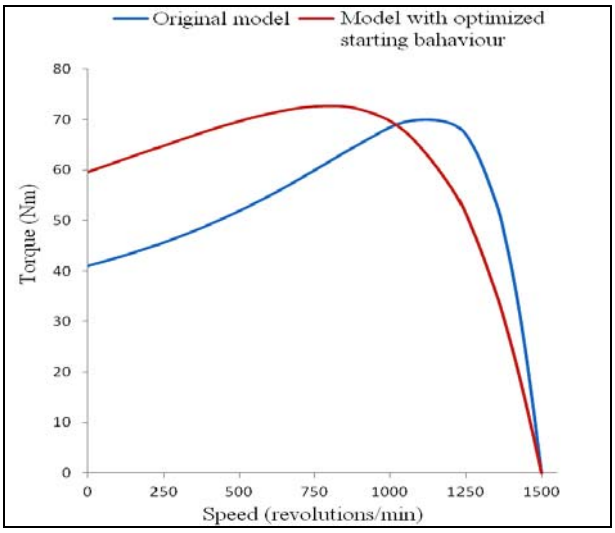

Fig. 7 Torque versus speed characteristics for the two models studied.

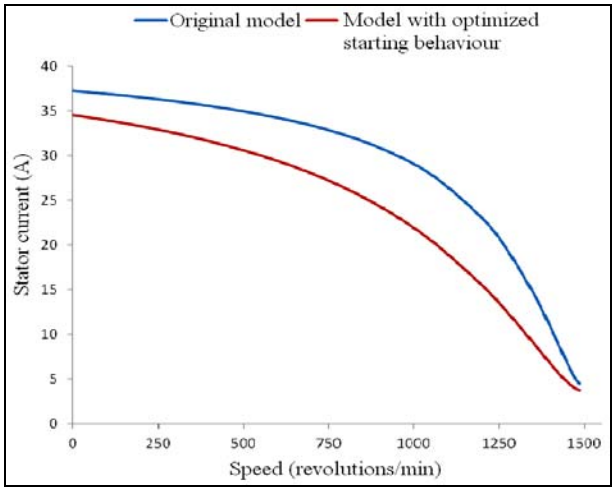

Fig. 8 Stator current versus speed characteristics for the two models studied.

4. Optimization of the Motor's Output Power

In this case, the model that occurred from the optimization process, presents maximized output power at nominal speed. The optimization analysis takes into account all the geometric variables of the rotor. The model in which this optimization case has lead, is presented in Fig. 9.

The comparative geometric rotor variables of the original model and the model with maximized output power are presented in Table 3. The depth of the rotor bar, as a consequence of the changes in A and B variables, has been increased. The width of the rotor

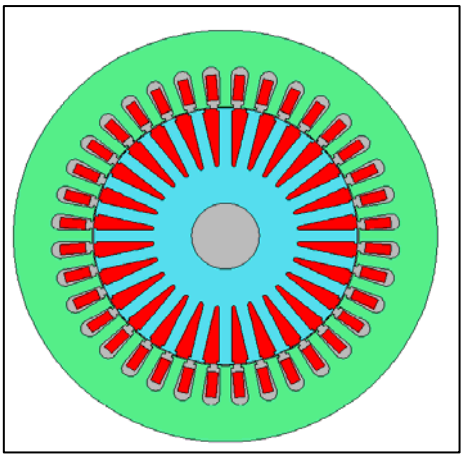

Fig. 9 The model with optimized output power at nominal speed.

Table 3 The geometric rotor variables of the original and the optimized model.

Design variables	A	B	C	D	E
Original model	35.35	2.2	3	1.5	1.1
Optimized model	29.65	2.03	2.53	1.21	0.89

bar, which depends on the variable C, has also increased. Both the variables D and E, which concern the rotor slot width and opening respectively, have been decreased. The changes in A, B and D design variables concern the bar resistance. The new optimized model has lower bar resistance. So, it is expected that this model's torque-speed characteristic would have been displaced to the right compared to the torque-speed characteristic of the original model.

The produced torque-speed and stator current-speed characteristics of both, the model with optimized output power and the original model are presented in Figs. 10 and 11, respectively. At starting, the optimized model presents 1.7% lower torque and 10.5% higher current than the original model. Furthermore, the pullout torque of the optimized model is higher and it occurs at higher speed than the original model. Finally, the stator current of the optimized model is greater for every speed as shown in Fig. 11.

5. Optimization of the Motor's Efficiency

In this paragraph, the target is to build a model of an induction motor with greater efficiency at nominal speed than the original. This is the primary goal of

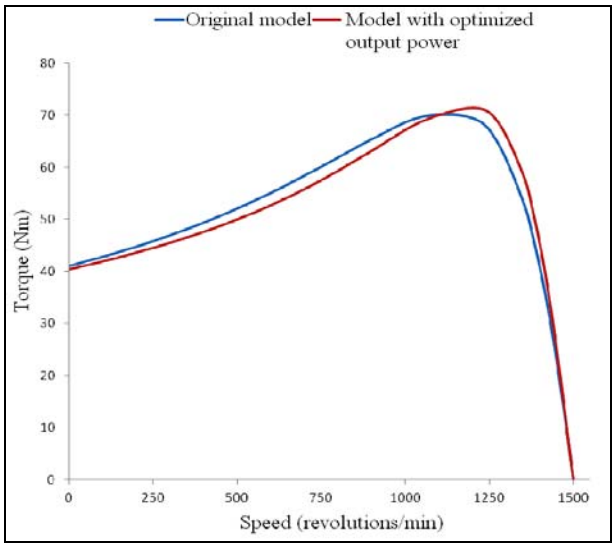

Fig. 10 Torque versus speed characteristics for the two models.

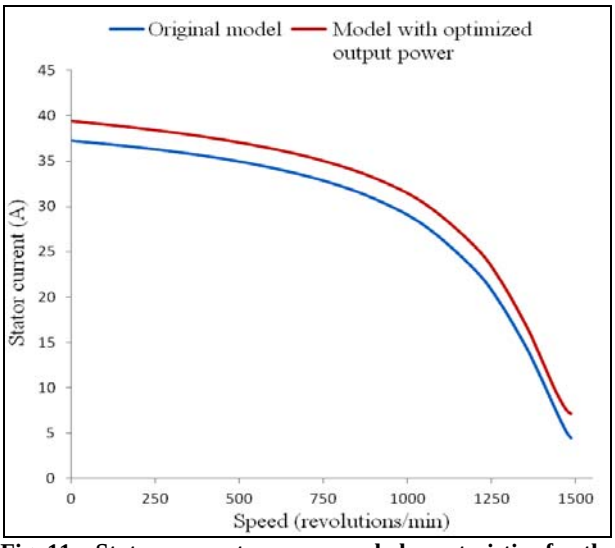

Fig. 11 Stator current versus speed characteristics for the two models.

electric motor designers worldwide due to the energy consuming synchronous reality. Although, an induction motor buyer has as priority to purchase the product cheaply, the user is also trying to run the motor with the least expense. The fact is that, the choice of an energy saving induction motor will pay back its higher cost within two years. The optimization analysis of this section takes into account all the geometric variables of the rotor. After the optimization process, several models characterized by greater efficiency than the original model, have been created and are presented in Table 4. The model chosen to be the product of this

optimization case is Model 4 which presented in Fig. 12. The choice of Model 4 as the best solution, depends on its output power which is only 3.5% reduced compared to the output power of the original model (4,055.34 W), while its efficiency has increased at about 5% (the original model's efficiency was 80.49). Finally, the input power of the optimized model is about 9% less than the original model's, showing perfectly that the optimized model is less energy consuming. Of course, the choice of the authors in this case has been arbitrary. Under general investigation, the choice of the best optimized solution is strongly dependant on the application of the motor.

The comparative geometric rotor variables of the original model and the model with optimized efficiency at nominal speed are presented in Table 5. The depth of the rotor bar, as a consequence of the changes in A and B variables, has been increased. The width of the rotor bar, which depends on the variable C, has decreased. Both the variables D and E, which concern the rotor slot width and opening respectively, have been increased.

The comparative produced torque-speed and stator current-speed characteristics of the model with optimized output power and the original model are presented in Figs. 13 and 14 respectively. At starting, the optimized model presents both lower torque and starting current than the original model. Furthermore, the pullout torque of the optimized model is lower and

Table 4 Characteristics of the models with optimized efficiency at nominal speed.

	Torque (Nm)	Input Power (W)	Output power (W)	cosφ	Efficiency (%)
Model 1	25.49	4481.93	3840.96	0.82	85.70
Model 2	24.64	4312.64	3713.93	0.81	86.12
Model 3	24.27	4232.03	3657.08	0.81	86.41
Model 4	25.98	4586.72	3914.96	0.82	85.35
Model 5	23.91	4159.48	3603.18	0.80	86.63
Model 6	26.26	4675.39	3957.25	0.82	84.64
Model 7	27.31	5013.95	4115.13	0.82	82.07

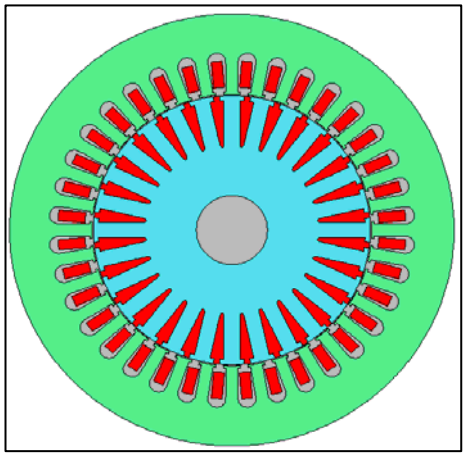

Fig. 12 The model with optimized efficiency at nominal speed.

Table 5 The geometric rotor variables of the original and the model with optimized efficiency.

Design variables	A	B	C	D	E
Original model	35.35	2.2	3	1.5	1.1
Optimized model	33.81	2.34	3.14	1.98	1.6

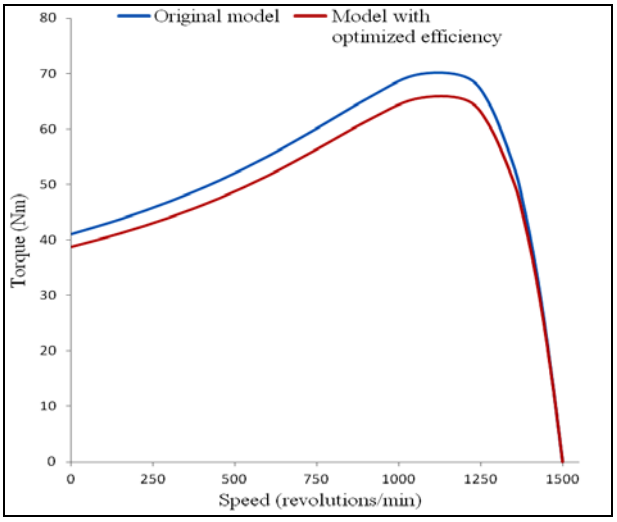

Fig. 13 Torque versus speed characteristics for the two models examined.

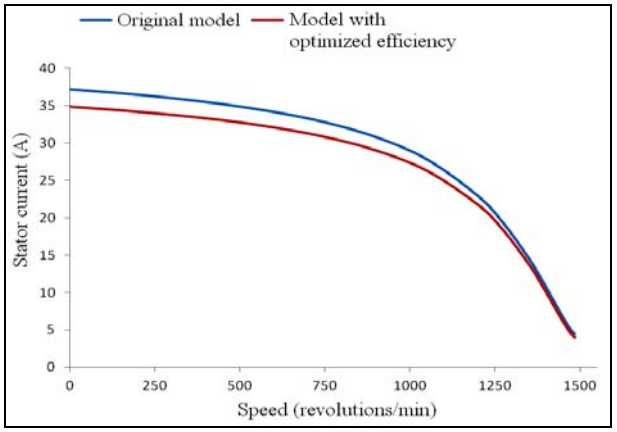

Fig. 14 Stator current versus speed characteristics for the two models examined.

Table 6 The electromagnetic characteristics of the models created and studied.

models	Original model	Model – Optimized starting	Model – Optimized output power	Model – Optimized efficiency
Starting Torque (Nm)	41.04	59.57	40.34	38.74
Starting Stator Current (A)	37.23	34.54	39.43	34.85
Torque at nominal speed (Nm)	26.91	15.85	29.73	25.98
Stator Current at nominal speed (A)	7.54	4.97	9.62	6.95
Input Power (W)	5038.14	2821.36	6061.89	4586.72
Output Power (W)	4055.34	2388.60	4480.31	3914.96
Power factor cosφ	0.83	0.71	0.78	0.82
Efficiency η (%)	80.49	84.66	73.9	85.35

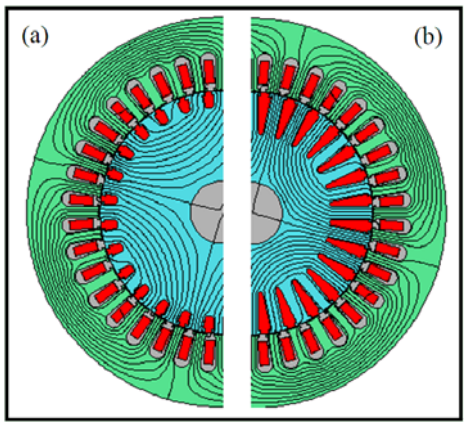

Fig. 15 Comparative spatial distribution of the magnetic flux at 1,485 rpm, for the cases: (a) model with optimized starting behaviour and (b) original model.

it occurs at higher speed than the original model. Finally, the stator current of the optimized model is lower for every speed as it can be seen in Fig. 14.

6. Comparative Characteristics of the Models Examined

In Table 6, the most important electromagnetic features of the models studied in this paper, are presented.

From the contents of Table 6, one can see that the main goals of the three separate optimization processes have been achieved. Moreover, one should observe that the power factors of all produced models are less than the original model's. Worst case is the model with optimized starting behaviour. The power factor is connected to the leakage magnetic flux. While the leakage resistance increases, the power factor is reduced. FEM is a useful tool in this case as it can present accurately the magnetic fields in the motor. In Fig. 15, the spatial distribution of the magnetic flux at 1,485 rpm, is presented for the cases of the motor with optimized starting behaviour (Fig. 15a) and the original model (Fig. 15b). It is obvious that the magnetic flux lines of the original model penetrate deep into the rotor core and as a consequence produce greater electromagnetic torque.

7. Conclusions

In this work, an asynchronous motor has been simulated as a parameterized model. The original model is optimized under three different functional criteria. The geometric features of the rotor are the optimization processes variables. Three new models have been created. The first model was optimized at starting. The model in which the first optimization process concluded, presents greater starting torque and less starting current than the original model. The second optimization process, leads to a model with greater output mechanical power. Finally, the third optimization case was carried out under the criteria of the improvement of the motor's efficiency. This optimized model presents 5% greater efficiency than the original model and about the same output power. This paper presents the advantage of the use of FEM tools for new electric motor design and the fast production of motors under special functional requirements, by manufacturers and industries.

Acknowledgments

The authors would like to thank the Research Committee of the University of Patras, for funding the

above work through the Research Program: "K. KARATHEODORIS 2010".

References

[1] J.F. Fuchsloch, W.R. Finley, R.W. Walter, The next generation motor, IEEE Industry Applications Magazine (2008) 37-43.

[2] A. Boglietti, A. Cavagnino, L. Ferraris, M. Lazzari, Energy-efficient motors, IEEE Industrial Electronics Magazine (2008) 32-37.

[3] A.H. Bonnett, Understanding the changing requirements and opportunities for improvement of operating efficiency of AC motors, IEEE Transactions on Industry Applications 29 (3) (1993) 600-610.

[4] A.Z. Bazghaleh, M.R. Naghashan, M.R. Meshkatoddini, , Optimum design of single-sided linear induction motors for improved motor performance, IEEE Transactions on Magnetics 46 (11) (2010) 3939-3947.

[5] D.A. Kohabas, Novel winding and core design for maximum reduction of harmonic magnetomotive force in AC motors, IEEE Transactions on Magnetics 45 (2) (2009) 735-745.

[6] S. Williamson, C.I. McClay, Optimization of the geometry of closed rotor slots for cage induction motors, IEEE Transactions on Industry Applications 32 (3) (1996) 560-568.

[7] M. Centner, U. Schafer, Optimized design of high-speed induction motors in respect of the electrical steel grade, IEEE Transactions on Industrial Electronics 57 (1) (2010) 288-295.

[8] A.H. Isfahani, B.M. Ebrahimi, H. Lesani, Design optimization of a low-speed single-sided linear induction motor for improved efficiency and power factor, IEEE Transactions on Magnetics 44 (2) (2008) 266-272.

[9] J. Kappatou, K. Gyftakis, A. Safacas, Fem study of the rotor slot design influences on the induction machine characteristics, Studies in Applied Electromagnetics and Mechanics, Advanced Computer Techniques in Applied Electromagnetics, IOS Press 30 (2008) 247-252.

[10] NEMA, Energy Management Guide For Selection and Use of Fixed Frequency Medium AC Squirrel-Cage Polyphase Induction Motors, NEMA Standards Publication MG 10-2001.